ELSEVIER

International Journal of Heat and Fluid Flow 19 (1998) 374–381

International Journal of HEAT AND FLUID FLOW

Effect on noncondensable gas on laminar film condensation along a vertical plate fin

Han-Taw Chen *, Shiuh-Ming Chang, Zen Lan

Department of Mechanical Engineering, National Cheng Kung University, Tainan 701, Taiwan ROC

Received 7 February 1997; accepted 12 December 1997

Abstract

Laminar film condensation along a vertical plate fin in the presence of a noncondensable gas is numerically investigated. In the present analysis, the gas mass fraction and temperature at the liquid–vapor interface is regarded as the spatial variation along the fin surface. Governing boundary layer equations together with their corresponding boundary conditions for the condensation system and the one-dimensional fin heat conduction equation with its negligible tip leakage are cast into dimensionless forms. The resulting system of equations is solved by using the central finite-difference approximation for the fin and local nonsimilarity method for boundary layer equations. Results show that the fin efficiency decreases with increasing the thermal resistance ratio of fin-to-liquid Nc, and relatively small amounts of the noncondensable gas in the bulk of the vapor have a significant effect on the fin efficiency for small values of Nc. In addition, the interface temperature is not equal to the fin temperature along the vertical fin, and the local heat transfer coefficient is not uniform, either.

Keywords: Noncondensable gas; Film condensation; Fin efficiency

Notation

c_L	similarity variable, $\{((\rho_L-\rho_v)g_aL^3)/(4\nu_L^2\rho_L)\}^{1/4}$
c_m	similarity variable, $(\Omega g_aL^3/(4\nu_m^2))^{1/4}$
c_{pL}	specific heat of condensate, J kg^{-1} C^{-1}
D_m	mass diffusivity, m^2 s^{-1}
E	fin efficiency, $0.375Q^*(\mathrm{Ja}/\mathrm{Pr}_L)^{1/4}$
f, F	reduced stream functions
g_a	gravitational acceleration, m s^{-2}
h_{fg}	latent heat of condensate, J kg^{-1}
h_{iso}	heat transfer coefficient for a pure saturated vapor, $(4k_Lc_L/(3L))(\mathrm{Pr}_L/\mathrm{Ja})^{1/4}$, W m^{-2} C^{-1}
h^*	dimensionless local heat transfer coefficient, $-\xi^{-1/4}[(\partial\theta/\partial\eta_L)/\theta]_{\eta_L=0}$
Ja	Jakob number, $c_{pL}(T_\infty-T_0)/h_{fg}$
k	thermal conductivity, kg m s^{-3}C^{-1}
L	fin length, m
$\dot{m}$	condensation rate per unit area, kg m^{-2}s^{-1}
Nc	thermal resistance ratio of fin-to-liquid, $Lk_Lc_L/(k_ft)$
Pr	Prandtl number, ν/α
p	total pressure of the system, atm
p_{vi}	vapor pressure at the interface, atm
$q^*(x)$	dimensionless local heat flux, $qL/(k_Lc_L(T_0-T_\infty))$
Q^*	dimensionless total heat flux, $QL/(k_Lc_L(T_0-T_\infty))$
Sc	Schmidt number, ν_m/D_m
T	condensate temperature, C
T_f	fin temperature, C
T_i	interface temperature, C
T_m	temperature in the vapor–gas layer, C
T_0	base temperature of the fin, C
t	half thickness of the fin, m
u, v	condensate velocities in the x- and y-directions, m s^{-1}
u_m, v_m	mixture velocities in the x- and y-directions, m s^{-1}
W_g	gas mass fraction, ρ_g/ρ_m
W_{gi}	gas mass fraction at the interface
$W_{g\infty}$	bulk mass fraction of gas
W_v	vapor mass fraction, ρ_v/ρ_m
x, y	Cartesian coordinates, m

Greek

ρ	condensate density, kg m^{-3}
μ	dynamic viscosity, kg m^{-1} s^{-1}
ν	kinematic viscosity, m^2 s^{-1}
ξ	dimensionless variable, x/L
η_L	similarity variable, $c_Ly/(L\xi^{1/4})$
η_m	similarity variable, $c_m(y-\delta)/(L\xi^{1/4})$
θ	dimensionless condensate temperature, $(T-T_\infty)/(T_0-T_\infty)$
θ_m	dimensionless temperature in the vapor–gas layer, $(T_m-T_\infty)/(T_0-T_\infty)$
ϕ	mass fraction difference, $W_g-W_{g\infty}$
ψ_L	reduced stream function for the condensate, $4\nu_Lc_L\xi^{3/4}f(\xi,\eta_L)$
ψ_m	reduced stream function for the vapor–gas mixture, $4\nu_mc_m\xi^{3/4}F(\xi,\eta_m)$
α	thermal diffusivity, m^2 s^{-1}
Ω	constant, $(M_g-M_v)/(M_g-(M_g-M_v)W_{g\infty})$

* Corresponding author.

0142-727X/98/$19.00
PII: S0142-727X(98)10002-4

Subscripts

f	fin
g	noncondensable gas
i	interface
L	condensate
m	mixture
v	vapor
∞	bulk

1. Introduction

The use of condensing fins is very extensive in the applications of heat exchange. To investigate heat-transfer characteristics of a condensing fin, the conjugate problem with the boundary layer equations on the condensation side and the fin heat conduction equation must simultaneously be considered. However, only a few investigators (Acharya et al., 1986; Burmeister, 1982; Lienhard and Dhir, 1974; Nader, 1978; Patankar and Sparrow, 1979; Sarma et al., 1988) studied laminar film condensation on a vertical fin. In these works, the saturated vapor did not contain the noncondensable gas. Patankar and Sparrow (1979) solved the coupled problem of condensation on an extended surface. Lienhard and Dhir (1974) investigated the case of laminar film condensation on various geometries without considering the effect of the interfacial resistance. Acharya et al. (1986) proposed two simpler methods to calculate the fin efficiency of laminar film condensation on various fin shapes. Sarma et al. (1988) studied laminar film condensation on a vertical plate fin with the variable thickness. Recently, Chen et al. (1994) applied the central finite-difference approximation and the local nonsimilarity method (Sparrow and Yu, 1971) to calculate the fin efficiency of a vertical condensing fin for a pure saturated vapor.

It is well known that the presence of a noncondensable gas in the bulk of the vapor can significantly lower the condensation rate below that for a pure vapor. An early experimental study by Othmer (1929) has shown that the heat transfer may be reduced by 50% or more due to the existence of a very small amount of air in the bulk of the vapor. Sparrow and coworkers (Sparrow and Lin, 1964; Minkowycz and Sparrow, 1966) have successfully applied boundary layer approximations to analyze the problem of condensation from a vapor–gas mixture on an isothermal vertical surface in the absence of forced convection. Their numerical results showed that the presence of a very small amount of a noncondensable gas in the bulk of the vapor could cause a large buildup of the noncondensable gas at the liquid–vapor interface. This buildup will lead to the reduction of the partial pressure of the vapor at the interface. The predicted results of Sparrow and Lin (1964) agreed with the experimental results given by Othmer (1929). However, the effects of temperature on the mixture density and heat transfer in the vapor–gas mixture were not considered in the work of Sparrow and Lin (1964). Sleger and Seban (1970) compared their experimental results with the numerical results given by Minkowycz and Sparrow (1966). They found that the measured condensation rates were about 20 percent above the predictions given by Minkowycz and Sparrow (1966). In these works (Sparrow and Lin, 1964; Minkowycz and Sparrow, 1966), the ripples at the liquid–vapor interface were not considered. Fujii et al. (1992) applied the similarity method to solve the two-phase boundary layer equations for free-convection condensation of an air–steam mixture on a vertical flat surface in the bulk air concentration range from 0.18 to 0.98 at 100 kpa. Recently, Coney et al. (1989) theoretically investigated the performance of a cooled longitudinal fin in a moist airflow. Panchal (1993) developed a simplified method to calculate the fin efficiency for condensation of a vapor in the presence of noncondensable gases. It is found from this work that heat- and mass-transfer coefficients are assumed constant along the fin surface. At the same time, the interface temperature is also assumed equal to the fin temperature in their calculation procedure. This assumption implies that the temperature drop across the liquid film is negligible.

The present study is concerned with laminar film condensation along a vertical plate fin in the presence of a noncondensable gas. In the present study, the one-dimensional fin heat conduction equation and boundary layer equations for liquid and vapor–gas regions must simultaneously be solved. It should be noted that the gas mass fraction W_{gi} and temperature T_i at the liquid–vapor interface are not known a priori for the present problem and must be determined as parts of the solution. Obviously, the calculation of the fin efficiency for the present study is more difficult than that for condensation in the absence of a noncondensable gas (Chen et al., 1994). It can be found from the work of Minkowycz and Sparrow (1966) that the effect of thermal diffusion and diffusional conduction on the local wall heat flux played a negligible role in the condensation of steam when air was regarded as a noncondensable gas. Based on this reason, the effect of thermal diffusion and diffusional conduction on the fin efficiency will not be considered in the present study. The main purpose of the present study is to investigate the effect of Nc and the amount of the noncondensable gas in the bulk of the vapor $W_{g\infty}$ on the fin efficiency.

2. Mathematical formulation

A schematic diagram of the physical model with the coordinate system is shown in Fig. 1. A vertical plate fin of thickness $2t$ and length L ($L \gg t$) is attached to a wall at temperature T_0 and is placed in the vapor containing a noncondensable gas. Far away from the fin, the vapor–gas mixture has a prescribed temperature T_∞ and a prescribed gas mass fraction $W_{g\infty} \cdot T_\infty$ is assumed to exceed T_0. The total pressure of the vapor–gas mixture is p. Due to the action of gravity, a continuous laminar film of condensate flows downward along the fin in a steady state. The velocity of the vapor–gas mixture in the x-direction approaches zero at some distance away from the liquid–vapor interface. Consequently, there simultaneously exist liquid and vapor–gas boundary layers. Assume that the effect of thermal diffusion and diffusional conduction is negligible, and the condensate along the vertical fin forms a laminar, nonrippling film. In addition, some assumptions made in the analysis for the isothermal case (Sparrow and Lin, 1964) are also applied to analyze the present problem. To further reduce the real problem to a soluble problem, the effect of condensate drainage characteristics on the fin efficiency will be neglected. It is worth mentioning that this consideration was not taken in the works of Coney et al. (1989) and Panchal (1993). Due to the above assumptions, the boundary layer equations expressing the conservation of mass, momentum, energy and species in the liquid and vapor–gas layers are respectively given:

Liquid layer:

$$\frac{\partial u}{\partial x}+\frac{\partial v}{\partial y}=0, \tag{1}$$

$$u\frac{\partial u}{\partial x}+v\frac{\partial u}{\partial y}=g_a\left(1-\frac{\rho_v}{\rho_L}\right)+\nu_L\frac{\partial^2 u}{\partial y^2}, \tag{2}$$

$$u\frac{\partial T}{\partial x}+v\frac{\partial T}{\partial y}=\alpha_L\frac{\partial^2 T}{\partial y^2}, \tag{3}$$

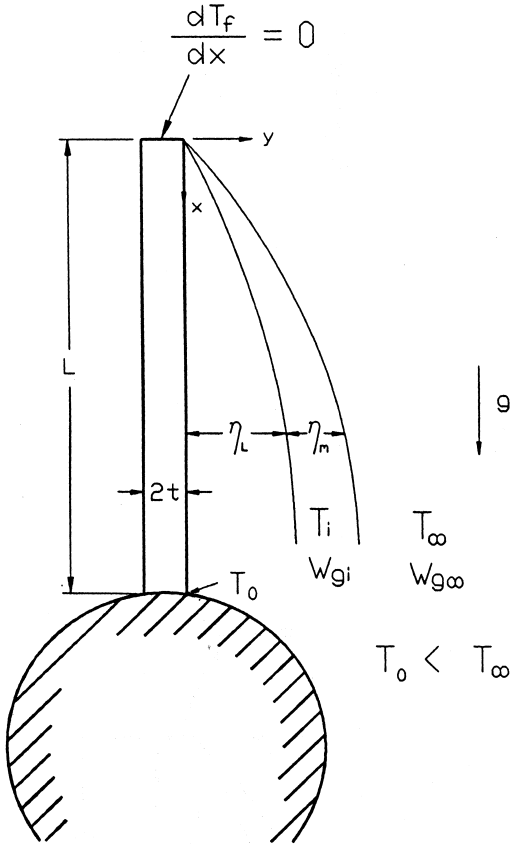

Fig. 1. Schematic representation of the system.

where x and y are Cartesian coordinates; u and v denote the velocity components of the condensate in the x- and y- directions, respectively; T is the condensate temperature; g_a is the gravitational acceleration; ρ_L and ρ_v are the densities of the condensate and the vapor, respectively; ν_L is the kinematic viscosity of the condensate; α_L is the thermal diffusivity of the condensate. The variation of fluid properties is neglected, and the viscous dissipation term is omitted from the energy equation since it is negligibly small.

Vapor–gas layer: If a noncondensable gas is present, the boundary layer equations in the vapor–gas region can be written as (Sparrow and Lin, 1964):

$$\frac{\partial u_m}{\partial x}+\frac{\partial v_m}{\partial y}=0, \tag{4}$$

$$u_m\frac{\partial u_m}{\partial x}+v_m\frac{\partial u_m}{\partial y}=g_a\left(1-\frac{\rho_\infty}{\rho_m}\right)+\nu_m\frac{\partial^2 u_m}{\partial y^2}, \tag{5}$$

$$u_m\frac{\partial W_g}{\partial x}+v_m\frac{\partial W_g}{\partial y}=D_m\frac{\partial^2 W_g}{\partial y^2}, \tag{6}$$

$$u_m\frac{\partial T_m}{\partial x}+v_m\frac{\partial T_m}{\partial y}=\alpha_m\frac{\partial^2 T_m}{\partial y^2}, \tag{7}$$

where u_m and v_m denote the velocity components of the vapor–gas mixture in the x- and y-directions, respectively; T_m is the temperature of the vapor–gas mixture; W_g is the gas mass fraction; ρ_∞ and ρ_m are the bulk density and the density of the vapor–gas mixture, respectively; D_m is the mass diffusivity; ν_m is the kinematic viscosity of the vapor–gas mixture; α_m is the thermal diffusivity of the vapor–gas mixture. It should be noted that fluid properties in the vapor–gas region correspond to average mixture properties.

The mass fractions of gas and vapor can be expressed as

$$W_g=\frac{\rho_g}{\rho_m},\qquad W_v=\frac{\rho_v}{\rho_m},$$
$$\rho_m=\rho_v+\rho_g,\qquad W_g+W_v=1, \tag{8}$$

where W_v is the vapor mass fraction and ρ_g is the density of the noncondensable gas.

The term $1-\rho_\infty/\rho_m$ can be obtained from the work of Sparrow and Lin (1964) as

$$1-\rho_\infty/\rho_m=\Omega(W_g-W_{g\infty}), \tag{9}$$

where

$$\Omega=\frac{M_g-M_v}{M_g-(M_g-M_v)W_{g\infty}},$$

$W_{g\infty}$ is the gas mass fraction far away from the liquid–vapor interface.

The boundary conditions for the boundary layer equations are

$$u=v=0,\quad T=T_f(x)\qquad \text{at } y=0, \tag{10a}$$

$$u_m\to 0,\quad T_m\to T_\infty,\quad W_g\to W_{g\infty}\qquad \text{as } y\to\infty, \tag{10b}$$

$$u=0\qquad \text{at } x=0,\quad y\geqslant 0, \tag{10c}$$

where T_f and T_∞ denote the fin temperature and the bulk temperature, respectively.

In order to complete the formulation of the problem, it is necessary to provide the following compatibility requirements. These compatibility requirements at the liquid–vapor interface, $y=\delta$, are the no-slip condition, shear force continuity, mass conservation, energy conservation, phase equilibria and interface impermeable to the noncondensable gas. They can be expressed as

$$u=u_m, \tag{11a}$$

$$\dot m=\rho_L\left(u\frac{d\delta}{dx}-v\right)=\rho_m\left(u_m\frac{d\delta}{dx}-v_m\right), \tag{11b}$$

$$\mu_L\frac{\partial u}{\partial y}=\mu_m\frac{\partial u_m}{\partial y}, \tag{11c}$$

$$T=T_m=T_i(x), \tag{11d}$$

$$W_g=W_{gi}(x) \tag{11e}$$

and

$$k_L\frac{\partial T}{\partial y}\bigg|_{y=\delta}-k_m\frac{\partial T_m}{\partial y}\bigg|_{y=\delta}=\dot m\,h_{fg}\quad \text{at } y=\delta, \tag{11f}$$

where $\dot m$ is the condensation rate per unit area; μ_L and μ_m denote the dynamic viscosities of the condensate and the vapor–gas mixture. The film thickness of the condensate δ is not known a priori and is one of the result of the present study.

The diffusive transport of gas, j_g, can be expressed as

$$j_g=-\rho_m D_m\frac{\partial W_g}{\partial y}. \tag{12}$$

Due to the fact that the interface is impermeable to the noncondensable gas, it follows that the interfacial mass flux of the noncondensable gas is zero. This impermeability condition can be written as

$$\rho_g\left(u_m\frac{d\delta}{dx}-v_m\right)-j_g=0\quad \text{at } y=\delta. \tag{13}$$

However, it should be noted that the interface temperature $T_i(x)$ in Eq. (11d) and the gas mass fraction at the interface $W_{gi}(x)$ are two important unknowns of the present problem.

The one-dimensional heat conduction equation for a thin fin with its negligible tip leakage of heat can be written as

$$\frac{d^2T_f(x)}{dx^2}=\frac{h(x)}{k_f t}(T_f(x)-T_\infty), \tag{14}$$

where k_f is the thermal conductivity of the fin and $h(x)$ is the local heat transfer coefficient based on the difference of the fin temperature and the bulk temperature. Eq. (14) is subjected to the following boundary conditions:

$$\frac{dT_f}{dx}=0 \quad \text{at } x=0, \tag{15a}$$

$$T_f=T_0 \quad \text{at } x=L. \tag{15b}$$

3. Local nonsimilarity method

The continuity Eqs. (1) and (4) can be satisfied by introducing stream functions ψ_L and ψ_m, where $u=\partial\psi_L/\partial y$, $v=-\partial\psi_L/\partial x$, $u_m=\partial\psi_m/\partial y$ and $v_m=-\partial\psi_m/\partial x$. The remaining differential equations and boundary conditions must be provided because the local nonsimilarity method will be applied to solve the present problem. To do this, a dimensionless coordinate ξ is first introduced as

$$\xi=x/L. \tag{16}$$

In addition, the dimensionless constants c_L and c_m, similarity variables η_L and η_m, reduced stream functions f and F, mass fraction difference ϕ and dimensionless temperatures θ and θ_v are also defined as follows:

Liquid layer:

$$c_L=\{((\rho_L-\rho_v)g_aL^3)/(4\nu_L^2\rho_L)\}^{1/4}, \qquad \eta_L=(c_Ly)/(L\xi^{1/4}),$$

$$\psi_L=4\nu_Lc_L\xi^{3/4}f(\xi,\eta_L), \qquad \theta=(T-T_\infty)/(T_0-T_\infty). \tag{17}$$

Vapor–gas layer:

$$c_m=(\Omega g_aL^3/(4\nu_m^2))^{1/4}, \qquad \eta_m=(c_m(y-\delta))/(L\xi^{1/4}),$$
$$\phi=W_g-W_{g\infty},$$

$$\psi_m=4\nu_mc_m\xi^{3/4}F(\xi,\eta_m), \qquad \theta_m=(T_m-T_\infty)/(T_0-T_\infty). \tag{18}$$

Substituting Eqs. (17) and (18) into Eq. (11b) in conjunction with the definition of the stream functions ψ_L and ψ_m yields

$$\dot m=\rho_Lc_L\nu_L\left(4\xi\frac{\partial f}{\partial\xi}+3f\right)\Big/(L\xi^{1/4})$$
$$=\rho_mc_m\nu_m\left(4\xi\frac{\partial F}{\partial\xi}+3F\right)\Big/(L\xi^{1/4}). \tag{19}$$

Due to the introduction of the above parameters, the momentum, energy and diffusion equations for the liquid and vapor–gas layers can be transformed into a set of the dimensionless forms:

$$f'''+3ff''-2(f')^2+1=4\xi(f'S'-f''S), \tag{20}$$

$$\theta''/\mathrm{Pr}_L+3f\theta'=4\xi(f'\varphi-\theta'S), \tag{21}$$

$$F'''+3FF''-2(F')^2+\phi=4\xi(F'G'-F''G), \tag{22}$$

$$\theta_m''/\mathrm{Pr}_m+3F\theta_m'=4\xi(F'\varphi_m-\theta_m'G), \tag{23}$$

$$\phi''/\mathrm{Sc}+3F\phi'=4\xi(F'\gamma-\phi'G), \tag{24}$$

where $S=\partial f/\partial\xi$, $\varphi=\partial\theta/\partial\xi$, $G=\partial F/\partial\xi$, $\varphi_m=\partial\theta_m/\partial\xi$ and $\gamma=\partial\phi/\partial\xi$; Pr_L is the condensate Prandtl number; Pr_m is the vapor–gas Prandtl number and Sc is the Schmidt number. They are defined as

$$\mathrm{Pr}_L=\nu_L/\alpha_L, \qquad \mathrm{Pr}_m=\nu_m/\alpha_m, \qquad \mathrm{Sc}=\nu_m/D_m. \tag{25}$$

Eqs. (20)–(24) together with their corresponding boundary conditions can approximately be solved by using the local nonsimilarity method at the second-level (Sparrow and Yu, 1971). On the other hand, terms involving $\partial S/\partial\xi$, $\partial\varphi/\partial\xi$, $\partial G/\partial\xi$, $\partial\varphi_m/\partial\xi$ and $\partial\gamma/\partial\xi$, etc., must be ignored. To this end, Eqs. (20)–(24) will be transformed into ten ordinary differential equations, parameterized in ξ. Five additional differential equations are obtained by differentiating Eqs. (20)–(24) with respect to ξ and are written as

$$S'''+3fS''+7Sf''-8f'S'=4\xi[(S')^2-S''S], \tag{26}$$

$$\varphi''/\mathrm{Pr}_L+3f\varphi'+7S\theta'-4f'\varphi=4\xi(S'\varphi-\varphi'S), \tag{27}$$

$$G'''+\gamma+3FG''+7GF''-8F'G'=4\xi[(G')^2-G''G], \tag{28}$$

$$\varphi_m''/\mathrm{Pr}_m+3F\varphi_m'+7G\theta_m''-4F'\varphi_m=4\xi(G'\varphi_m-\varphi_m'G), \tag{29}$$

$$\gamma''/\mathrm{Sc}+3F\gamma'+7G\phi'-4F'\gamma=4\xi(G'\gamma-\gamma'G). \tag{30}$$

The boundary conditions corresponding to Eqs. (20)–(24) and Eqs. (26)–(30) are

$$f=f'=S=S'=0, \quad \theta=\theta_f \qquad \text{at } \eta_L=0, \tag{31}$$

$$f'=F'\Omega^{1/2}, \qquad (4\xi G+3F)\Omega^{1/4}=R(4\xi S+3f),$$

$$F''\Omega^{3/4}=Rf'', \qquad G\Omega^{1/4}=RS, \qquad G'\Omega^{1/2}=S',$$

$$G''\Omega^{3/4}=RS'', \quad \theta=\theta_i, \quad \phi=\phi_i \qquad \text{at } \eta_L=\eta_{L\delta}, \tag{32}$$

$$\theta_m\to0, \quad \phi\to0, \quad F'\to0, \quad G'\to0 \qquad \text{as } \eta_m\to\infty, \tag{33}$$

where $\theta_f=(T_f-T_\infty)/(T_0-T_\infty)$, $\theta_i=(T_i-T_\infty)/(T_0-T_\infty)$ and $R=((\rho_L\mu_L)/(\rho_m\mu_m))^{1/2}$. The primes denote differentiation with respect to η_L for the liquid layer and to η_m for the vapor–gas layer.

Substituting Eqs. (17)–(19) into Eq. (11f) can yield the dimensionless equation of the energy balance at the liquid–vapor interface as

$$\mathrm{Ja}=-\mathrm{Pr}_L(3f+4\xi S)\left/\left(\theta'-\frac{k_mc_m\theta_m'}{k_Lc_L}\right)\right. \quad \text{at } \eta_L=\eta_{L\delta}, \tag{34}$$

where Ja is the Jakob number and is defined as $\mathrm{Ja}=c_{pL}(T_\infty-T_0)/h_{fg}$.

Substituting Eq. (12) into Eq. (13) in conjunction with Eqs. (18) and (19) yields

$$\phi'=-\mathrm{Sc}(3F+4\xi G)(\phi+W_{g\infty}) \quad \text{at } \eta_m=0. \tag{35}$$

Differentiating Eq. (35) with respect to ξ yields

$$\gamma'=-7G\mathrm{Sc}(\phi+W_{g\infty})-\mathrm{Sc}(3F+4\xi G)\gamma \quad \text{at } \eta_m=0. \tag{36}$$

It is evident that the system of Eqs. (20)–(24) and (26)–(30) together with boundary conditions (31)–(33) and (34)–(36) constitutes a mathematical form for laminar film condensation of a mixture steam along the vertical plate fin. However, the solution of the boundary layer equations can be obtained when $\theta_f(\xi)$ is specified.

The thermal coupling between the conduction equation and the energy equation in the liquid layer is expressed by the requirement that the temperature and heat flux must be continuous at the fin–liquid interface. These conditions are given as

$$T_f(x)=T(x,0) \tag{37}$$

and

$$-k_L \left.\frac{\partial T}{\partial y}\right|_{y=0} = h(x)(T_f(x) - T_\infty). \tag{38}$$

The substitution of Eqs. (16), (17) and (38) and the definition of θ_f in Eq. (31) into Eqs. (14), (15a) and (15b) can yield

$$\frac{d^2\theta_f(\xi)}{d\xi^2} = h^*(\xi)\mathrm{Nc}\theta_f(\xi) \tag{39}$$

and

$$\frac{d\theta_f}{d\xi} = 0 \quad \text{at } \xi = 0, \tag{40a}$$

$$\theta_f = 1 \quad \text{at } \xi = 1, \tag{40b}$$

where Nc can be regarded as the thermal resistance ratio of fin-to-liquid. h^* denotes the dimensionless local heat transfer coefficient. They are defined as

$$\mathrm{Nc} = \frac{L}{k_f t} k_L c_L \tag{41}$$

and

$$h^* = \frac{hL}{k_L c_L} = -\xi^{-1/4}\left[\frac{\partial\theta}{\partial\eta_L}\Big/\theta\right]_{\eta_L=0} = -\xi^{-1/4}\left[\frac{\partial\theta}{\partial\eta_L}\right]_{\eta_L=0}\Big/\theta_f(\xi). \tag{42}$$

The relation between the gas mass fraction at the liquid–vapor interface W_{gi} and the partial pressure of the vapor p_{vi} can expressed as (Sparrow and Lin, 1964)

$$p_{vi}/p = (1 - W_{gi})/(1 - W_{gi}(1 - M_v/M_g)). \tag{43}$$

Due to the fact that the liquid–vapor interface is a saturation state, the relation between the interface temperature T_i and the interfacial vapor pressure p_{vi} for water vapor can be expressed as

$$T_i = \frac{3968}{11.92 - \ln(p_{vi})} - 232.9. \tag{44}$$

Eq. (44) fits the data listed in the Steam Tables of the saturated water to an accuracy of ±5% for $5^\circ\mathrm{C} \leqslant T_i \leqslant 374.14^\circ\mathrm{C}$.

It is seen that $\xi = 0$ is a singular point for the present problem. To overcome this difficulty in the numerical calculation, we assume that the variation in $[\partial\theta/\partial\eta_L]_{\eta_L=0}$ from $\xi = 0$ to $\xi = \Delta\xi$ is small. Integration of Eq. (39) from $\xi = 0$ to $\xi = \Delta\xi$ in conjunction with Eqs. (40a) and (42) yields the approximate values of $d\theta_f/d\xi$ and θ_f at $\xi = \Delta\xi$ as

$$\left.\frac{d\theta_f}{d\xi}\right|_{\xi=\Delta\xi} = \frac{4}{3}\mathrm{Nc}\left[-\frac{\partial\theta}{\partial\eta_L}\right]_{\eta_L=0}(\Delta\xi)^{3/4} \tag{45}$$

and

$$\theta_f|_{\xi=\Delta\xi} = \frac{16}{21}\mathrm{Nc}\left[-\frac{\partial\theta}{\partial\eta_L}\right]_{\eta_L=0}(\Delta\xi)^{7/4} + \theta_f(0). \tag{46}$$

The discretized form of Eq. (39) in the interval $\Delta\xi \leqslant \xi \leqslant 1$, using the central finite-difference algorithm, is

$$\frac{\theta_{f,i+1} - 2\theta_{f,i} + \theta_{f,i-1}}{(\Delta\xi)^2} = \mathrm{Nc}h_i^*\theta_{f,i}, \quad i = 1, 2, \ldots, n-1, \tag{47}$$

where $\theta_{f,0} = \theta_f(0)$ will be guessed, $\theta_{f,n} = \theta_f(1) = 1$, $h_i^* = h^*(i/n)$, n denotes the nodal number in the fin.

4. Solution procedures

The computational procedures of the present problem are listed in the following.

1. The initial guesses of $\theta_f(0)$ and $\eta_{L\delta}(\Delta\xi)$ are first given for the given set $(T_0, T_\infty, \mathrm{Pr_L}, \mathrm{Ja}, \mathrm{Pr_m}, k_m/k_L, c_m/c_L, \mathrm{Sc}, R, p, L, \mathrm{Nc}$ and $W_{g\infty})$. Thus, the values of $d\theta_f/d\xi$ and θ_f at $\xi = \Delta\xi$ can be obtained from Eqs. (45) and (46). At the same time, the boundary layer equations (20)–(24) and (26)–(30) together with boundary conditions (31)–(33) and (34)–(36) can be solved by using the fourth-order Runge–Kutta method in conjunction with the Nachtsheim–Swigert iteration scheme (Adams and Rogers, 1973) to fulfil the boundary conditions at the vapor–gas interface. If the energy balance Eq. (34) at the liquid–vapor interface is not satisfied, a new guess for $\eta_{L\delta}(\Delta\xi)$ will again be made. The entire calculation is repeated until Eq. (34) is satisfied. Furthermore, values of $h^*(\Delta\xi)$ and $\eta_{L\delta}(\Delta\xi)$ can be obtained from these computational procedures.
2. Values of $h^*(\Delta\xi)$ and $\theta_f(\Delta\xi)$ obtained from step 1 are used as input data for determining results at the next location. The results of $d\theta_f/d\xi$ and θ_f at $\xi = 2\Delta\xi$ can be obtained from Eq. (47). However, $h^*(2\Delta\xi)$ must be determined from boundary layer equations. These computational processes are continued until $\xi = 1$.
3. The secant method is applied to determine the approximate value of $\theta_f(0)$ using the calculated results of $\theta_f(1)$ obtained from two different initial guesses of $\theta_f(0)$. Steps 1 and 2 are repeated later until $|\theta_{f,\mathrm{cal}}(\xi = 1) - 1| < 10^{-3}$.

The local heat flux along the condensing fin $q(x)$ can be expressed as

$$q(x) = -k_L \left.\frac{\partial T}{\partial y}\right|_{y=0} = h(x)(T_f(x) - T_\infty). \tag{48}$$

Substituting Eqs. (16) and (17) into Eq. (48) yields the dimensionless form of $q(x)$ as

$$q^*(\xi) = \frac{qL}{k_L c_L(T_0 - T_\infty)} = -\xi^{-1/4}\left[\frac{\partial\theta}{\partial\eta_L}\right]_{\eta_L=0}. \tag{49}$$

The numerical values of the overall fin heat transfer rate Q can be obtained by integrating $q(x)$ over the condensing fin. However, all of the heat lost by the fin must be conducted into the fin base at $x = L$, Thus, Q can be written as

$$Q = -2k_f t \left.\frac{dT_f}{dx}\right|_{x=L} = 2k_L \int_0^L \left(\frac{\partial T}{\partial y}\right)_{y=0} dx. \tag{50}$$

The dimensionless form of Q can be written as

$$Q^* = \frac{Q}{k_L c_L(T_\infty - T_0)} = \frac{2}{\mathrm{Nc}}\left[\frac{d\theta_f}{d\xi}\right]_{\xi=1}. \tag{51}$$

Assume that the fin efficiency E is defined as the ratio of the actual condensation taking place on the fin to the condensation rate estimated from the isothermal surface maintained at its base temperature T_0 and the classical Nusselt model in the absence of the noncondensable gas. Thus, the fin efficiency E can be written as

$$E = -k_f t \left.\frac{dT_f}{dx}\right|_{x=L} \Big/ (h_{\mathrm{iso}} L(T_\infty - T_0)), \tag{52}$$

where h_{iso} denotes the heat transfer coefficient at the isothermal condition for a pure saturated vapor and is given as

$$h_{\mathrm{iso}} = (4k_L c_L/(3L))(\mathrm{Pr_L}/\mathrm{Ja})^{1/4}. \tag{53}$$

The substitution of Eqs. (50), (51) and (53) into Eq. (52) gives

$$E = 0.375Q^*(\mathrm{Ja}/\mathrm{Pr_L})^{1/4}. \tag{54}$$

For the convenience of numerical analysis, $M_g, M_v, \mathrm{Pr_L}$, $\mathrm{Ja}, \mathrm{Pr_m}, R, \mathrm{Sc}, p, L, T_0$ and T_∞ are taken as $M_g = 28.97$, $M_v = 18.02, \mathrm{Pr_L} = 2.57$, $\mathrm{Ja} = 0.11, \mathrm{Pr_m} = 1.09$, $k_m/k_L = 0.024$,

$c_m/c_L = 52.41$, $R = 228.7, Sc = 0.59, p = 1$ atm, $L = 0.03$ m, $T_0 = 40°C$ and $T_\infty = 100°C$.

5. Results and discussion

Fig. 2 shows the distributions of ϕ_i $(= W_{gi} - W_{g\infty})$ along the vertical plate fin for various $W_{g\infty}$ values and $Nc = 3$. Thus, the buildup amount of the noncondensable gas at the liquid–vapor interface W_{gi} along the fin can be obtained from Fig. 2. It can be observed from Fig. 2 that very high concentrations of the noncondensable gas build up at the interface even though there are very small amount of the noncondensable gas in the bulk. This result agrees with that shown in the work of Sparrow and Lin (1964). Fig. 2 also implies that increasing the value of $W_{g\infty}$ can lead to the increase in the amount of W_{gi}. On the other hand, the increase in the value of $W_{g\infty}$ will cause the increase in the buildup amount of the noncondensable gas at the interface along the condensing fin. Such a buildup of the noncondensable gas will lead to the reduction of the vapor pressure at the interface. It can be found from Eq. (44) that the increase in the value of $W_{g\infty}$ will cause the decrease in the interface temperature T_i and the thermal driving force $(T_i - T_0)$. This result is shown in Fig. 3. In turn, it also lowers condensation heat transfer due to the decrease of the interface temperature T_i. This important finding is that the interface temperature T_i decreases along the fin and is not equal to the fin temperature. The above statement implies that the assumption of $T_f = T_i$ proposed by Coney et al. (1989) and Panchal (1993) seems to be not very reasonable. It can be seen from Figs. 3 and 5 that the difference between T_f and T_i increases along the fin for a fixed $W_{g\infty}$ value and decreases with increasing the value of $W_{g\infty}$.

Fig. 4 shows the distributions of the dimensionless local heat flux q^* along the fin for various $W_{g\infty}$ values and $Nc = 3$. It is seen that the area under the q^*-curve increases with decreasing the value of $W_{g\infty}$. On the other hand, the increase in the value of $W_{g\infty}$ can lead to the decrease in the overall heat transfer rate Q^*.

The distributions of the dimensionless fin temperature θ_f for various $W_{g\infty}$ values and $Nc = 3$ are presented in Fig. 5. This figure shows that the value of the fin temperature gradient at $\xi = 1$ increases with decreasing the value of $W_{g\infty}$. Moreover, based on the definition of θ_f, the above result also implies that

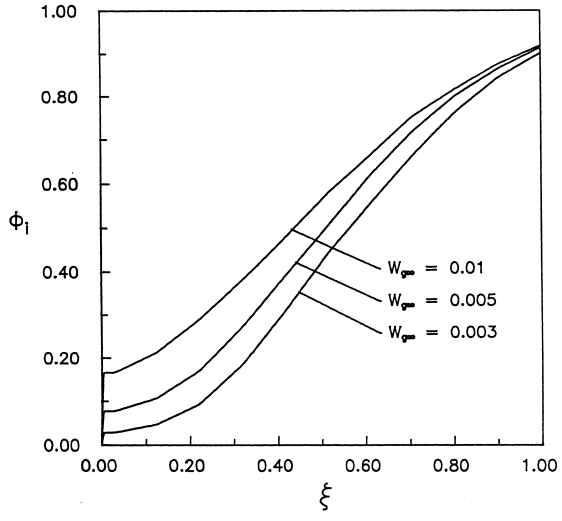

Fig. 2. Distributions of ϕ_i along the fin for various $W_{g\infty}$ values and $Nc = 3$.

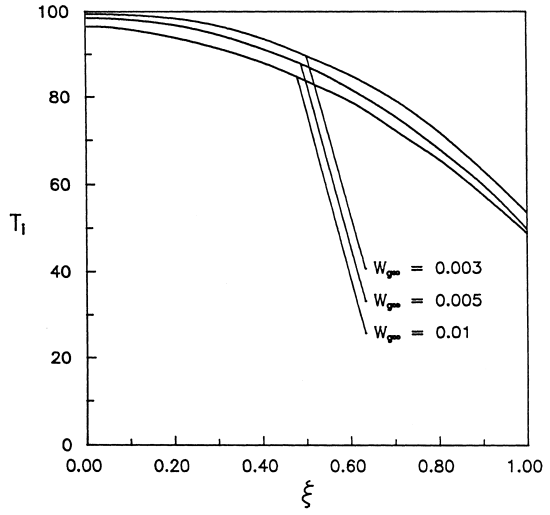

Fig. 3. Distributions of T_i along the fin for various $W_{g\infty}$ values and $Nc = 3$.

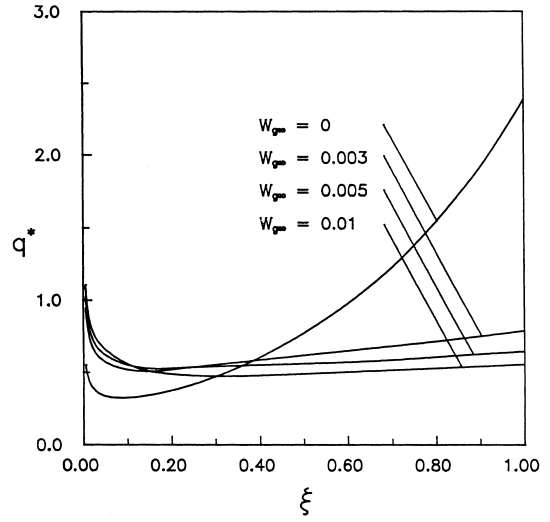

Fig. 4. Distributions of q^* along the fin for various $W_{g\infty}$ values and $Nc = 3$.

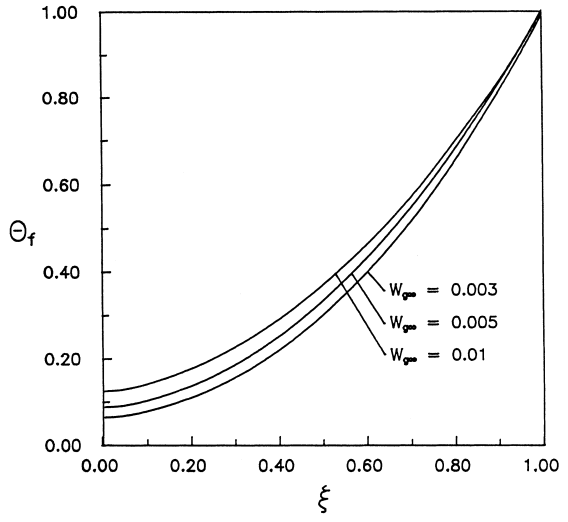

Fig. 5. Distributions of θ_f for various $W_{g\infty}$ values and $Nc = 3$.

the smaller the value of $W_{g\infty}$, the higher the tip temperature of the fin.

Fig. 6 illustrates the distributions of the dimensionless local heat transfer coefficient h^* along the condensing fin for various $W_{g\infty}$ values and Nc = 3. It is seen that the value of h^* is not constant along the vertical fin and decreases with increasing the value of $W_{g\infty}$. Obviously, this result is different from the assumption made by Coney et al. (1989) and Panchal (1993). Another interesting observation is that the area under the h^*-curve increases with decreasing the value of $W_{g\infty}$. This phenomenon is similar to the figure of the q^*-curve.

The distributions of q^* along the fin for various Nc values and $W_{g\infty} = 0.003$ are plotted in Fig. 7. The physical significance of Nc indicates that the increase of Nc can be regarded as the increase of the fin thermal resistance. This statement implies that the heat lost by the fin will decrease with increasing the Nc value. Thus, the increase in the value of Nc can cause the decrease in the area under the q^*-curve and makes the fin temperature become more nonisothermal, as shown in Figs. 7 and 8. On the other hand, decreasing the value of Nc can lower

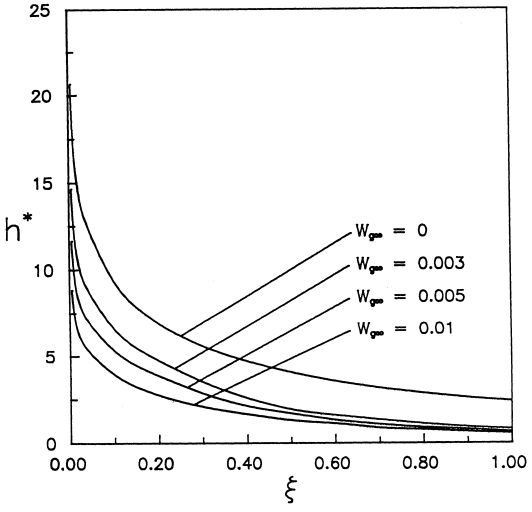

Fig. 6. Distributions of h^* along the fin for various $W_{g\infty}$ values and Nc = 3.

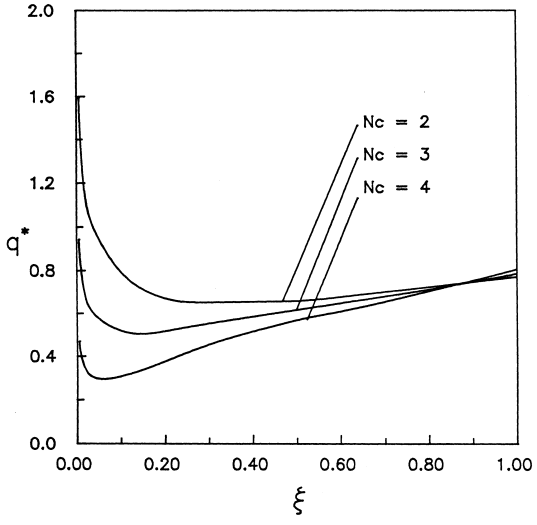

Fig. 7. Distributions of q^* along the fin for various Nc values and $W_{g\infty} = 0.003$.

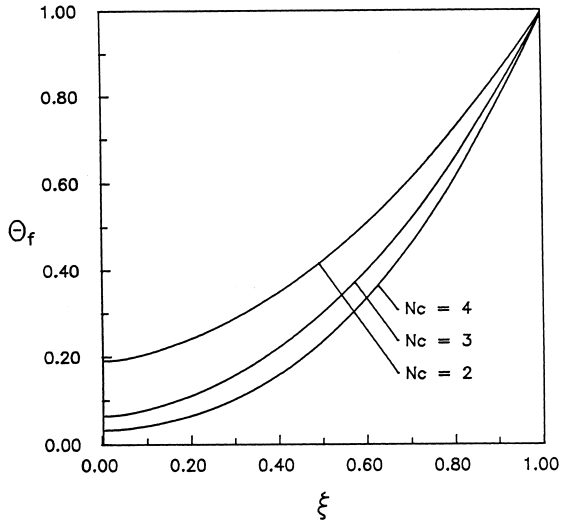

Fig. 8. Distributions of θ_f for various Nc values and $W_{g\infty} = 0.003$.

the tip temperature of the fin and leads to the increase in the value of the fin temperature gradient at $\xi = 1$.

The variation of the fin efficiency E with $W_{g\infty}$ for Nc = 3 is shown in Fig. 9. It is seen that the fin efficiency decreases with increasing the value of $W_{g\infty}$ because increasing $W_{g\infty}$ can lead to the decrease in condensation heat transfer. The fin efficiency for $W_{g\infty} = 0.004$ is about 33.3% lower than that for $W_{g\infty} = 0$ and is about 12.7% higher than that for $W_{g\infty} = 0.01$. Obviously, the variation of E in the range $0 \leqq W_{g\infty} \leqq 0.004$ is greater than that in the range $0.004 \leqq W_{g\infty} \leqq 0.01$ for Nc = 3. The above results show that a small amount of a noncondensable gas in the bulk of the vapor can cause the significant reduction of the fin efficiency. The variation of E with Nc for various $W_{g\infty}$ values is shown in Fig. 10. The fin efficiency decreases with increasing the value of Nc. It can be observed from Fig. 10 that the reductions in the fin efficiency is about 29.2% for Nc = 0.4 and $W_{g\infty} = 0.003$ and is about 15.5% for Nc = 0.4 and $W_{g\infty} = 0.001$. In addition, the difference of the fin efficiency between Nc = 0.4 and Nc = 2.0 is about 45.6% for $W_{g\infty} = 0.001$ and is about 40.3% for $W_{g\infty} = 0.003$. It is expected because the increase of Nc can be regarded as the increase of the fin thermal resistance. Thus, decreasing the value of Nc can also lead to the significant reduction in the fin efficiency.

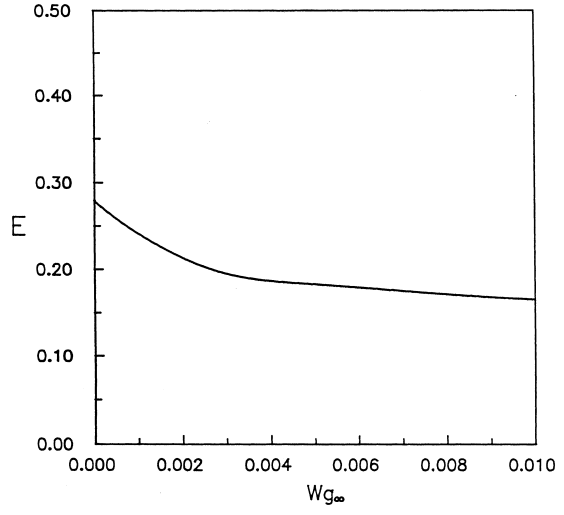

Fig. 9. Variation of E with $W_{g\infty}$ for Nc = 3.

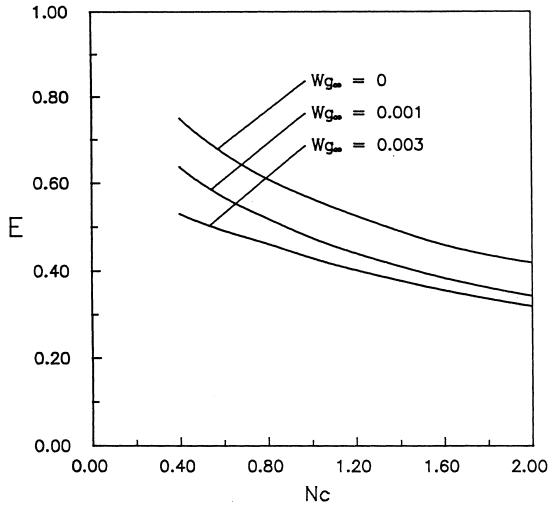

Fig. 10. Variation of E with Nc for various $W_{g\infty}$ values.

6. Conclusions

The present study applies the local nonsimilarity method and the central finite-difference method to solve the problem of laminar film condensation along a vertical plate fin in the presence of a noncondensable gas. Results show that the dimensionless local heat transfer coefficient is not constant along the fin, and its value decreases with increasing the value of $W_{g\infty}$. In addition, the fin efficiency increases with decreasing the value of $W_{g\infty}$ or Nc. The presence of a small amount of the noncondensable gas gives rise to a marked reduction in the fin efficiency, especially for small Nc values, and the effect of Nc on the fin efficiency is also pronounced. The difference between the interface temperature and the fin temperature increases along the condensing fin and decreases with increasing the value of $W_{g\infty}$.

References

Acharya, S., Braud, K.G., Attar, A., 1986. Calculation of fin efficiency for condensing fins. Int. J. Heat Fluid Flow 7, 96–98.

Adams, J.A., Rogers, D.F., 1973. Computer-Aided Heat Transfer Analysis. McGraw-Hill, New York, pp. 393–403.

Burmeister, L.C., 1982. Vertical fin efficiency with film condensation. ASME J. Heat Transfer 104, 391–393.

Chen, H.T., Lan, Z., Wang, T.I., 1994. Study of conjugate conduction-laminar film condensation for a vertical plate fin. Int. J. Heat Mass Transfer 16, 2592–2597.

Coney, J.E.R., Sheppard, C.G.W., EI-Shafei, E.A.M., 1989. Fin performance with condensation from humid air: A numerical investigation. Int. J. Heat Fluid Flow 10, 224–231.

Fujii, T., Shinzato, K., Lee, J.B., 1992. Free-convection condensation of air–steam mixture on a vertical surface: Comparison between theory and experiment. Trans. JSME 58B (549), 1617–1623.

Lienhard, J.H., Dhir, V.K., 1974. Laminar film condensation on nonisothermal and arbitrary heat flux surfaces and on fins. ASME J. Heat Transfer 96, 197–203.

Minkowycz, W.J., Sparrow, E.M., 1966. Condensation heat transfer in the presence of noncondensables, interfacial resistance, superheating, variable properties and diffusion. Int. J. Heat Mass Transfer 9, 1125–1144.

Nader, W.K., 1978. Extended surface heat transfer condensation. In: Paper CS-5, Sixth International Heat Transfer Conference 2, Toronto, Canada, pp. 407–412.

Othmer, D.F., 1929. The condensation of steam. Indust. Eng. Chem. 21, 576–583.

Panchal, C.B., 1993. Fin efficiency calculation for condensation in the presence of noncondensable gases. In: Taborek, J. et al. (Eds.), Proceedings of The Engineering Foundation Conference on Condensation and Condenser Design, United Engineering Trustees, pp. 293–302.

Patankar, S.V., Sparrow, E.M., 1979. Condensation on an extended surface. ASME J. Heat Transfer 101, 434–440.

Sarma, P.K., Chary, S.P., Rao, V.D., 1988. Condensation on a vertical plate fin of variable thickness. Int. J. Heat Mass Transfer 31, 1941–1944.

Slegers, L., Seban, R.A., 1970. Laminar film condensation of steam containing small concentrations of air. Int. J. Heat Mass Transfer 13, 1941–1947.

Sparrow, E.M., Lin, S.H., 1964. Condensation heat transfer in the presence of a noncondensable gas. ASME J. Heat Transfer C86, 430–436.

Sparrow, E.M., Yu, H.S., 1971. Local nonsimilarity thermal boundary-layer solutions. ASME J. Heat Transfer 93, 328–334.